

# Analytical calculation of the solid angle subtended by a circular disc detector at a point cosine source<sup>\*</sup>

M. J. Prata<sup>1</sup>

*Instituto Tecnológico e Nuclear (ITN), Estrada Nacional 10, Sacavém 2686-953, Portugal*

---

## Abstract

We derive analytical expressions for the solid angle subtended by a circular disc at a point source with cosine angular distribution ( $f(\mu) = \mu$ ) under the sole condition that the disc lies in half-space illuminated by the source ( $\mu \geq 0$ ). The expressions are given with reference to two alternative coordinate systems (S and S'), S being such that the  $z$  axis is parallel to the symmetry axis of the disc and S' such that the  $z'$  axis is aligned with the source direction. Sample plots of the expressions are presented.

*Key words:* solid angle, point cosine source, disc detector, circular disc, analytic expressions

---

## 1 Introduction

In two previous works we obtained analytical expressions for the solid angle subtended by a cylindrical shaped detector at a point cosine source in the cases where the source axis is orthogonal (Prata, 2003a) or parallel (Prata, 2003c) to the cylinder axis of revolution. As ancillary results we also derived expressions for the solid angle defined by a circular disc in the cases where the source axis is orthogonal or parallel to the symmetry axis of the disc. Circular apertures are often considered in optics and radiation physics; and disc-shaped detectors

---

<sup>\*</sup> Partially supported by Fundação para a Ciência e Tecnologia (Programa Praxis XXI - BD/15808/98)

*Email address:* mjprata@sapo.pt (M. J. Prata).

<sup>1</sup> Tel.: +351-21-944-0690; fax: +351-21-846-3276.

are widely used in nuclear science (e.g. Neutron Activation Analysis). While the case of an isotropic source has been treated to great extent (Jaffey (1954), Macklin (1957), Masket *et al* (1956), Masket (1957), Gardner and Verghese (1971), Prata (2003b)), the case of a point cosine source has, to our best knowledge, deserved little attention. For these reasons, in the present work we extend the scope of our previous results by performing the calculation of the solid angle defined by a circular disc and a point cosine source pointing at an arbitrary direction, under the sole restriction that the disc lies in the half-space illuminated by the source.

The solid angle subtended by some surface at a point source considered at the origin can be defined by

$$\Omega_{surf} = \iint_{\substack{\text{directions} \\ \text{hitting surface}}} f(\boldsymbol{\Omega})d\Omega , \quad (1)$$

where  $f(\boldsymbol{\Omega})d\Omega$  is the source angular distribution. In the case of a point cosine the distribution is defined in relation to some direction axis specified by the unit vector  $\mathbf{k}$  and it is given by  $f(\boldsymbol{\Omega}) = (\boldsymbol{\Omega} \cdot \mathbf{k} + |\boldsymbol{\Omega} \cdot \mathbf{k}|)/(2\pi)$ , the  $(2\pi)^{-1}$  factor ensuring that  $0 \leq \Omega_{surf} \leq 1$ . For  $\mu = \boldsymbol{\Omega} \cdot \mathbf{k}$  it follows that  $f(\boldsymbol{\Omega}) = \{\mu/\pi (\mu \geq 0); 0 (\mu < 0)\}$  so that the source only emits into the hemisphere around  $\mathbf{k}$ . Because of this, the integration limits in the RHS of eq. 1 are to be determined from the conditions that  $\mu \geq 0$  and that each included  $\boldsymbol{\Omega}$  direction hits the surface. In the following we shall assume that the the position of disc is always chosen is such manner that  $\mu \geq 0$  for each point on the disc. This restriction greatly simplifies the calculation without, we believe, reducing the practical interest of the expressions. This is so because, in actual situations, the source is distributed over some planar surface; the source axis is coincident with the normal to the surface and then the restriction simply demands that the detector is held somewhere on the illuminated side of the radiating surface or eventually directly on the surface but does not intersect it.

## 2 Solid Angle Calculation

To proceed it is advantageous to consider two systems of coordinates (S and S') with a common origin also coincident with the source position. In the S' system (fig. 1) the  $z'$  axis is aligned with the source direction  $\mathbf{k}$ ; the center of the disc (C) is specified by  $h$  and  $R$ ; and the symmetry axis of the disc is described by the angles  $\beta$  and  $\gamma$ ,  $\beta$  being the angle between the source and the disc axis. When working in the S system (fig. 2), the  $z$  axis is parallel to the disc axis, C is located by means of  $L$  and  $d$ ; and  $\mathbf{k}$  is given by angles  $\beta$

and  $\alpha$ . From the symmetry of the source it is clear that the solid angle is an even function of  $\alpha$  or  $\gamma$  and in the following calculations we will thus assume that  $0 \leq \alpha \leq \pi$  and  $0 \leq \gamma \leq \pi$ . Also, it is sufficient to consider  $0 \leq \beta \leq \pi/2$ .

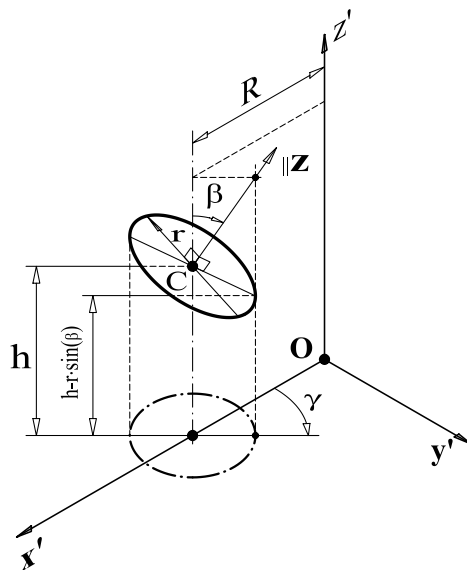


Fig. 1. Notation used in the  $S'$  coordinate system.

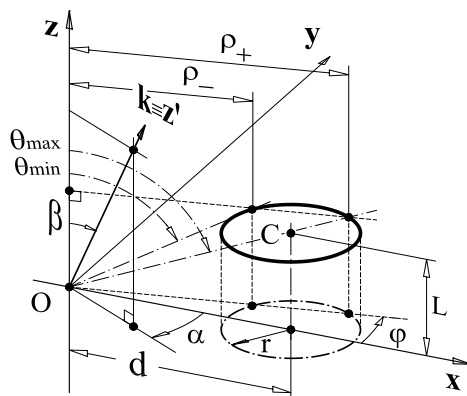


Fig. 2. Notation used in the  $S$  coordinate system.

The restriction that  $\mu \geq 0$  for the whole disc is easily expressed in  $S'$  by

$$h - r \cdot \sin \beta \geq 0 , \quad (2)$$

$r > 0$  being the disc radius. This is automatically satisfied, provided  $h \geq r$ , but otherwise, it further reduces the range of variation of  $\beta$  to

$$0 \leq \beta \leq \arcsin(h/r) , h < r . \quad (3)$$

It is readily found that the coordinates of a point in  $S'$  and  $S$  ( $\mathbf{P}'$  and  $\mathbf{P}$ ) are

related by an orthonormal matrix ( $\mathbf{M}$ ):

$$\mathbf{P}' = \mathbf{M} \cdot \mathbf{P} , \quad (4)$$

$$\mathbf{P} = \mathbf{M}^T \cdot \mathbf{P}' , \quad (5)$$

where  $\mathbf{M}$  is given by

$$\mathbf{M}(\gamma, \beta, \alpha) = \begin{bmatrix} \sin \gamma \sin \alpha + \cos \gamma \cos \beta \cos \alpha & \sin \gamma \cos \alpha - \cos \gamma \cos \beta \sin \alpha & -\cos \gamma \sin \beta \\ \cos \gamma \sin \alpha - \sin \gamma \cos \beta \cos \alpha & \cos \gamma \cos \alpha + \sin \gamma \cos \beta \sin \alpha & \sin \gamma \sin \beta \\ \sin \beta \cos \alpha & -\sin \beta \sin \alpha & \cos \beta \end{bmatrix} \quad (6)$$

and its inverse is given by the transpose

$$\mathbf{M}^T(\gamma, \beta, \alpha) = \begin{bmatrix} \sin \gamma \sin \alpha + \cos \gamma \cos \beta \cos \alpha & \cos \gamma \sin \alpha - \sin \gamma \cos \beta \cos \alpha & \sin \beta \cos \alpha \\ \sin \gamma \cos \alpha - \cos \gamma \cos \beta \sin \alpha & \cos \gamma \cos \alpha + \sin \gamma \cos \beta \sin \alpha & -\sin \beta \sin \alpha \\ -\cos \gamma \sin \beta & \sin \gamma \sin \beta & \cos \beta \end{bmatrix} . \quad (7)$$

Let  $(x_c, y_c, z_c)$  and  $(x'_c, y'_c, z'_c)$  denote the coordinates of the disk center in S and S', respectively. Because of the azimuthal symmetry of the source, it is possible to choose the  $x, y$  axes in each coordinate system so that  $y_c = y'_c = 0$ . Starting in the S system, setting  $(x_c, y_c, z_c) = (d, 0, L)$  and fixing  $\alpha$  and  $\beta$ , one then uses eq. 4 to obtain  $(x'_c, y'_c, z'_c)$ . The value of  $\gamma$  is determined by imposing that  $y'_c = 0$ , which gives

$$\tan \gamma = (d \sin \alpha) / (d \cos \beta \cos \alpha - L \sin \beta) , \quad (8)$$

or, for  $0 \leq \gamma \leq \pi$ ,

$$\begin{aligned} \gamma &= \gamma(\beta, L, d, \alpha) \\ &= \arccos[(d \cos \beta \cos \alpha - L \sin \beta) / \sqrt{(d \sin \alpha)^2 + (d \cos \beta \cos \alpha - L \sin \beta)^2}] . \end{aligned} \quad (9)$$

The values of  $h$  and  $R$  are obtained from

$$h = z'_c = h(\beta, L, d, \alpha) = d \sin \beta \cos \alpha + L \cos \beta , \quad (10)$$

and

$$R = x'_c = \sqrt{x_c'^2 + y_c'^2} \quad (11)$$

$$= R(\beta, L, d, \alpha) \quad (12)$$

$$= \sqrt{d^2(\sin^2 \alpha + \cos^2 \alpha \cos^2 \beta) + L^2 \sin^2 \beta - dL \sin(2\beta) \cos \alpha} . \quad (13)$$

Conversely, starting in the S' system with  $(x'_c, y'_c, z'_c) = (R, 0, h)$ , using eq. 5 to obtain  $(x_c, y_c, z_c)$  and imposing that  $y_c = 0$ , there results

$$\alpha = \alpha(\beta, h, R, \gamma) \quad (14)$$

$$= \arccos[(R \cos \beta \cos \gamma + h \sin \beta)] / \sqrt{(R \sin \gamma)^2 + (R \cos \beta \cos \gamma + h \sin \beta)^2} . \quad (15)$$

$$L = z_c = L(\beta, h, R, \gamma) = h \cos \beta - R \sin \beta \cos \gamma , \quad (16)$$

and

$$d = x_c = \sqrt{x_c^2 + y_c^2} \quad (17)$$

$$= d(\beta, h, R, \gamma) \quad (18)$$

$$= \sqrt{R^2(\sin^2 \gamma + \cos^2 \gamma \cos^2 \beta) + h^2 \sin^2 \beta + Rh \sin(2\beta) \cos \gamma} . \quad (19)$$

The substitution of the expression for  $h$  (eq. 10) on the RHS of eq. 2 and a bit of algebra gives the restriction  $\mu \geq 0$  expressed in terms of S variables:

$$L \geq (r - d \cos \alpha) \cdot \tan \beta . \quad (20)$$

If  $\beta = 0$ , the previous eq. can be rewritten as

$$\cos \alpha \geq r/d . \quad (21)$$

The solid angle (eq. 1) is best calculated in S. With the notation described in fig. 2, it is seen that  $\mathbf{k} = (\sin \beta \cos \alpha, -\sin \beta \sin \alpha, \cos \beta)$  and

$$\mathbf{k} \cdot \boldsymbol{\Omega} = \cos \beta \cos \theta + \sin \beta \sin \theta \cos(\alpha + \varphi) , \quad (22)$$

where, for a given direction,  $\theta$  is the polar angle from the  $z$  axis and  $\varphi$  is the azimuthal angle in the  $xy$  plane measured from the  $x$  axis. The solid angle is then given by

$$\Omega = \pi^{-1} \int_{\varphi_{\min}}^{\varphi_{\max}} \int_{\theta_{\min}}^{\theta_{\max}} \mathbf{k} \cdot \boldsymbol{\Omega} \sin(\theta) d\theta d\varphi , \quad (23)$$

Because the position of the disc is such that  $\mu \geq 0$  (eq. 20 or equivalently eq. 2), the integrations limits are determined only by the condition that each included  $(\theta, \varphi)$  direction hits the detector.

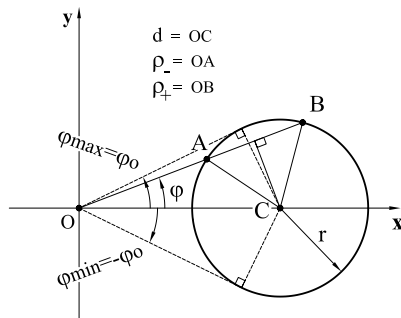


Fig. 3. Integrations limits for  $\varphi$  and definitions of  $\rho_{\pm}$ .

Referring to figs. 2 and 3, it follows that  $\varphi_{\max} = -\varphi_{\min} = \varphi_o \equiv \arcsin(r/d)$ ,

$$\theta_{\max} = \arccos(L/\sqrt{L^2 + \rho_+^2}),$$

$$\theta_{\min} = \arccos(L/\sqrt{L^2 + \rho_-^2}),$$

where

$$\rho_{\pm} = d \cos \varphi \pm \sqrt{r^2 - (d \sin \varphi)^2}.$$

Then,

$$\begin{aligned} \Omega &= \pi^{-1} \left( \cos \beta \int_{-\varphi_o}^{+\varphi_o} \int_{\theta_{\min}}^{\theta_{\max}} \cos \theta \sin \theta \, d\theta d\varphi + \right. \\ &\quad \left. \sin \beta \int_{-\varphi_o}^{+\varphi_o} \cos(\alpha + \varphi) \int_{\theta_{\min}}^{\theta_{\max}} \sin^2 \theta \, d\theta d\varphi \right), \end{aligned} \quad (24)$$

$$= \cos \beta \cdot \Omega_{\parallel} + \sin \beta \cdot \Omega_{\perp}, \quad (25)$$

where

$$\Omega_{\parallel} = \pi^{-1} \int_{-\varphi_o}^{+\varphi_o} \int_{\theta_{\min}}^{\theta_{\max}} \cos \theta \sin \theta \, d\theta d\varphi \quad (26)$$

and

$$\Omega_{\perp} = \pi^{-1} \int_{-\varphi_o}^{+\varphi_o} \cos(\alpha + \varphi) \int_{\theta_{\min}}^{\theta_{\max}} \sin^2 \theta \, d\theta d\varphi. \quad (27)$$

The values of  $\Omega_{\parallel}$  and  $\Omega_{\perp}$  were previously obtained. From Prata (2003c, eqs. 23

and 24)

$$\Omega_{\parallel}(L, d, r) = \frac{1}{2} \left[ 1 + \frac{1}{\sqrt{1-m^2}} \frac{(r^2 - d^2 - L^2)}{(r^2 + d^2 + L^2)} \right] \quad (28)$$

and from Prata (2003a, eqs. 20 and 55),

$$\Omega_{\perp}(L, d, r, \alpha) = \cos \alpha \frac{|L|}{2d} \left[ \frac{1}{\sqrt{1-m^2}} - 1 \right], \quad (29)$$

where

$$m = 2rd / (L^2 + d^2 + r^2). \quad (30)$$

In eq. 29 the absolute value of  $L$  is used since  $L$  is restricted only by eq. 20 and can thus be negative.

## 2.1 Special cases

We emphasize two cases: that where the axis of symmetry of the disc is parallel to that of the source ( $\beta = 0$ ) and the situation where the center of the disc is located on the source axis ( $R = 0$ ).

- When  $\beta = 0$ , from eqs. 9, 10 and 13 there results that  $\gamma = \alpha$ ,  $h = L$  and  $R = d$ . The same results could of course be obtained from 15, 16 and 19. The restriction imposed by either of the equivalent eqs. 20 or 2 gives  $L \geq 0$ . Using eqs. 25, 28 and 30 it is seen that the solid angle is independent from  $\alpha$  as expected and

$$\Omega(\beta = 0) = \Omega_{\parallel}(L, d, r) \quad (31)$$

It was shown in Prata (2003c) that  $\Omega_{\parallel}$  is continuous except for  $L \rightarrow 0$  since

$$\Omega_{\parallel}(L \rightarrow 0) = \{0 \ (d > r), 1/2 \ (d = r), 1 \ (d < r)\}. \quad (32)$$

- When  $R = 0$ , eqs. 15, 16 and 19 give  $\alpha = 0$ ,  $\forall \gamma$ ,  $L = h \cos \beta$  and  $d = h \sin \beta$ . Using eqs. 25, 28, 29 and 30, a little algebra yields

$$\Omega(R = 0) = \cos \beta \frac{r^2}{\sqrt{(r^2 + h^2 + 2rh \sin \beta)(r^2 + h^2 - 2rh \sin \beta)}}. \quad (33)$$

$\Omega(R = 0)$  is then independent from  $\gamma$ , as expected.

Eq. 33 can be approximated by

$$\Omega(R=0) = \left(\frac{r}{h}\right)^2 \cos \beta \left[ 1 - \left(\frac{r}{h}\right)^2 \cos 2\beta + \dots \right], r \ll h. \quad (34)$$

In the case where  $h = r$ , it is straightforward to simplify eq. 33 to:

$$\Omega(R=0, h=r) = 1/2, \forall \beta. \quad (35)$$

### 3 Results

Here we present sample plots of the solid angle. In the following we choose to work with S' parameters  $(\beta, h, R, \gamma)$  and consider throughout a disc of radius  $r = 1$ . We first address the case  $\beta = 0$ , so that  $\Omega = \Omega_{\parallel}$ ,  $L = h$  and  $d = R$ . As said before (section 2.1)  $\Omega$  is not continuous as  $L \rightarrow 0$ . This is illustrated in fig. 4 where  $\Omega$  is plotted as a function of  $h(L)$  for different  $R(d)$  values.

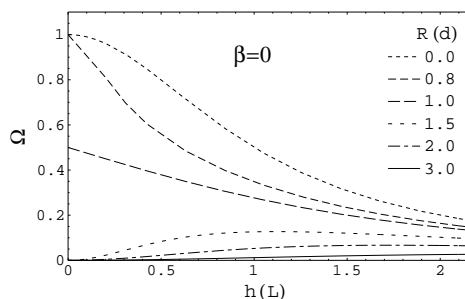


Fig. 4. Solid angle subtended by a disc of radius 1 with symmetry axis parallel to that of the source.

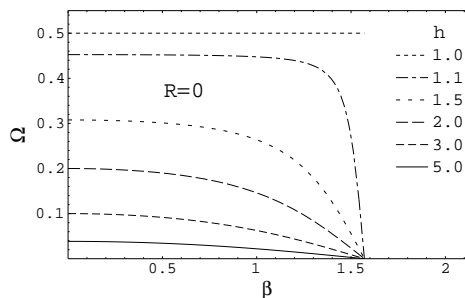


Fig. 5. Solid angle subtended by a disc of radius 1 and center located on the source axis.

In fig. 5 the situation where the disc center is on the source axis ( $R = 0$ ) is represented. Here,  $\Omega$  does not depend on  $\gamma$  (section 2.1) and plots of the solid angle as a function of  $\beta$  are shown for different  $h$  values, including the special case  $h = r$ , where  $\Omega = 1/2$ , regardless of  $\beta$ . To avoid restricting the range of variation of  $\beta$  (see eq. 3), the values of  $h$  were chosen such that  $h \geq r$ . In figs. 6, 7 and 8 the effect of offsetting the position of the disc center from the



source axis is shown for three offset values ( $R = h/4$ ,  $R = h/2$  and  $R = 3/4h$ ) and for two values of  $\beta$  ( $\pi/12$ ,  $\pi/6$ ). As argued before, the solid angle is an even function of  $\gamma$  and it is seen that for the larger tilting angle ( $\beta = \pi/6$ ) the dependence from  $\gamma$  is enhanced.

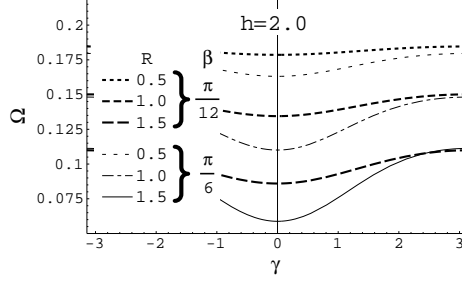


Fig. 6. Solid angle subtended by a disc of radius 1 with center with fixed  $h = 2$ .

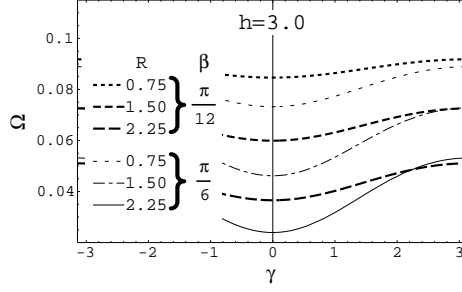


Fig. 7. Solid angle subtended by a disc of radius 1 with center with fixed  $h = 3$ .

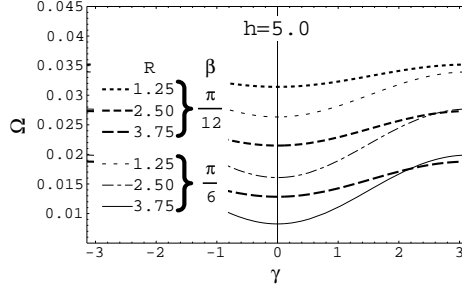


Fig. 8. Solid angle subtended by a disc of radius 1 with center with fixed  $h = 3$ .

When plotting  $\Omega$  as a function of  $\gamma$  while holding all other parameters constant, there *can* be a zero, i.e. a value of  $\gamma$  such that  $\Omega(\gamma_0) = 0$ . Looking at fig. 2 it is clear that  $\Omega = 0$  if  $L = 0$  and  $d > r$ . Setting  $L = 0$  in eq. 16 and solving for  $\gamma$  gives an equation for the zero,

$$\gamma_0 = \arccos[h/(R \tan \beta)] , \quad (36)$$

which has no solution for  $h/(R \tan \beta) > 1$ . Thus, this qualitative feature is dependent on the sign of  $h - R \cdot \tan \beta$ , which actually distinguishes the situations where the disc always presents the same face to the source from those where the face presented depends on the value of  $\gamma$ . This is schematically explained

in fig. 9 where the effect of changing  $\gamma$  from 0 to  $\pi$  is shown as seen in  $S'$  (see also fig.1), when looking along the  $y'$  axis. If  $h - R \cdot \tan \beta = 0$  (fig. 9a), the source always 'sees' the lower face of the disc and for  $\gamma = 0$  one has  $L = 0$  and, consequently,  $\Omega = 0$ . If  $h - R \cdot \tan \beta > 0$  (fig. 9b) the source always looks at the lower face of the disc but  $\Omega$  is never zero. Finally, for  $h - R \cdot \tan \beta < 0$  (fig. 9c), it is seen that, as the disc swirls with increasing  $\gamma$ , the upper face is first shown (e.g.  $\gamma = 0$ ) and then the lower face is presented (e.g.  $\gamma = \pi$ ), which means that  $\Omega = 0$  at some point in between. This behaviour is illustrated in fig. 10, for  $h = 2$  and  $\beta = \pi/3$ . The zero shows up for  $R \geq h/\tan \beta \simeq 1.16$ .

One should notice that in the preceding discussion it was implicitly assumed that  $d > r$  when  $\gamma = \gamma_0$ . We now proceed to show that eq. 2, in the strict form

$$h - r \cdot \sin \beta > 0 , \quad (37)$$

guarantees that  $d > r$ . Using eq. 36 to eliminate  $h$  in eqs. 37 and 19 gives

$$\cos \gamma \cdot R / \cos \beta > r \quad (38)$$

and

$$d = \sqrt{\cos^2 \gamma + \sin^2 \gamma \cos^2 \beta} R / \cos \beta . \quad (39)$$

respectively. Since  $\sqrt{\cos^2 \gamma + \sin^2 \gamma \cos^2 \beta} \geq \cos \gamma$  therefore  $d > r$ .

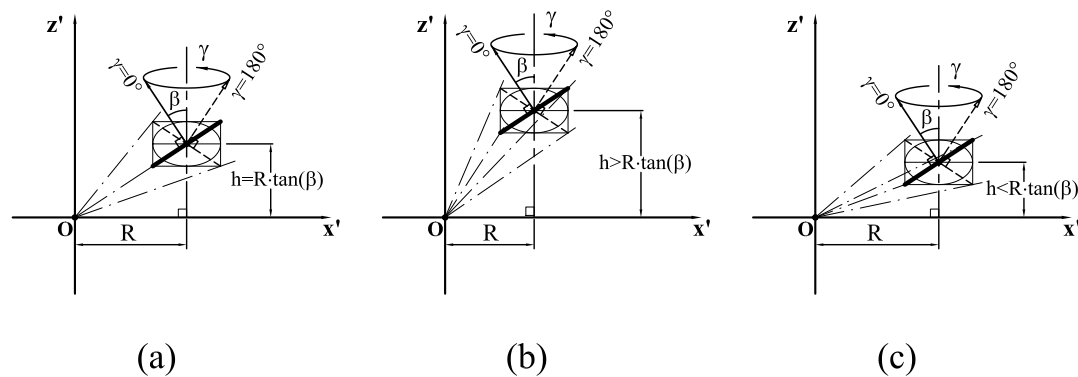


Fig. 9. The effect of changing  $\gamma$  as seen from a side view in the  $S'$  system for: (a)  $h = R \cdot \tan(\beta)$  , (b)  $h > R \cdot \tan(\beta)$  and (c)  $h < R \cdot \tan(\beta)$ .

## 4 Summary and Outlook

Analytical expressions for the solid angle subtended by a circular disc at a point cosine source were obtained , under the single restriction that the disc is located in the half-space illuminated by the source (eq. 2 or 20). It was shown

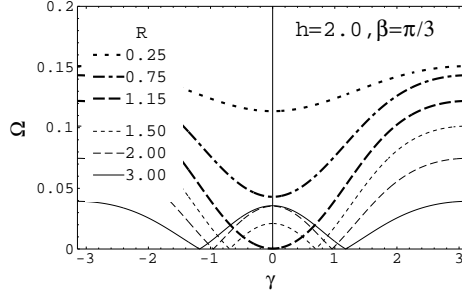


Fig. 10. Plots of  $\Omega$  as a function of  $\gamma$  showing a zero for  $h \leq R \cdot \tan(\beta)$ .

(eq. 24) that the solid angle can be decomposed into the combination of two components ( $\Omega_{\parallel}$  and  $\Omega_{\perp}$ ) corresponding to the situations where the symmetry axis of the disc is parallel or orthogonal to the source direction.  $\Omega$  can be calculated relatively to two alternative coordinate systems (S' and S) shown in figs. 1 and 2. The parameters pertaining to each system ( $\{\gamma, h, R, \beta, r\}$ ,  $\{\alpha, L, d, (\beta, r)\}$ ) are related by eqs. 9, 10, 13, 15, 16 and 19.

A similar calculation to that presented here can be performed for the solid angle defined by a cylindrical detector. A work where we report this latter result is in preparation.

## Acknowledgements

I would like to thank Professor John H. Hubbell for providing a copy of the works by A.V. Masket (Masket, 1957) and A.H. Jaffey (Jaffey, 1954). This work was partially supported by Fundação para a Ciência e Tecnologia (Grant BD/15808/98 - Programa Praxis XXI).

## References

- Gardner, R.P. & Verghese, K., 1971. On the solid angle subtended by a circular disc. Nucl. Instr. Meth. 93, 163-167.
- Jaffey, A.H., 1954. Solid angle subtended by a circular aperture at point and spread sources: formulas and some tables. Rev. Sci. Instr. 25 (4), 349-354.
- Macklin, P.A., 1957. Expression for the solid angle subtended by a circular disc at a point source in terms of elliptic integrals. Included as a footnote in Masket (1957).
- Masket, A.V., Macklin, R.L. & Schmitt, H.W., 1956. Tables of solid angle values and activations. ORNL-2170 (Oak Ridge Nat. Lab., Oak Ridge, Tenn.)
- Masket, A.V., 1957. Solid Angle contour integrals, series, and tables. Rev. Sci. Instr. 28 (3), 191-197.

- Prata, M.J., 2003a. Analytical calculation of the solid angle defined by a cylindrical detector and a point cosine source with orthogonal axes. *Rad. Phys. Chem.* 66 (6), 387-395. math-ph/0209065.
- Prata, M.J., 2003b. Solid angle subtended by a cylindrical detector at a point source in terms of elliptic integrals. Accepted for publication in *Rad. Phys. Chem.* (RPC2930). math-ph/0211061.
- Prata, M.J., 2003c. Analytical calculation of the solid angle defined by a cylindrical detector and a point cosine source with parallel axes. Submitted. math-ph/0302003.